Available online at www.sciencedirect.com

SCIENCE DIRECT®

Thin Solid Films 464–465 (2004) 175–179

thin solid films

www.elsevier.com/locate/tsf

In-situ transmission electron microscope observation of nitriding processes of titanium thin films by nitrogen-implantation

J.J. Wang[a], Y. Kasukabe[b,*], T. Yamamura[a], S. Yamamoto[c], Y. Fujino[b]

[a] Department of Metallurgy, Tohoku University, Aramaki-Aza-Aoba 02, Aoba, Sendai 980-8579, Japan
[b] International Student Center/Department of Electronic Engineering, Tohoku University, Kawauchi, Aoba, Sendai 980-8576, Japan
[c] Department of Material Development, Japan Atomic Energy Research Institute-Takasaki, 1233 Watanuki, Takasaki 370-1292, Japan

Available online 15 July 2004

Abstract

To clarify the "epitaxial" formation process of TiN films due to nitrogen-implantation, changes of crystallographic structures of as-deposited Ti films during N-implantation were studied by using a transmission electron microscope (TEM). Analysis of the results of TEM observations indicated that H atoms which constituted TiH_x were completely released from as-deposited Ti films when the films were heated up to 350 °C, and that the H-released unstable fcc-Ti sublattice was transformed into hcp-structure. Ions of N_2^+ with 62 keV were implanted into the hcp-Ti films held at 350 °C. In the N-implanted Ti film (N/Ti = 0.954), there coexisted NaCl-type TiN_y and a small amount of hcp-Ti. The (001)- and (110)-oriented TiN_y were "epitaxially" formed by the transformation of (03·5)- and ($\bar{2}$1·0)-oriented hcp-Ti, respectively. The lattice of N-implanted hcp-Ti was expanded by the occupation of octahedral sites by N atoms. Strain due to the lattice expansion was considered as a driving force for the hcp–fcc transformation of Ti sublattice.

PACS: 68.37.Lp.; 68.55.Jk.; 81.15.Aa.; 85.40.Ry.
Keywords: Ion-implantation; TiN; fcc–hcp transformation; In-situ TEM

1. Introduction

Titanium nitrides are non-stoichiometric compounds and show metallic, covalent and also ionic properties, which make them interesting from both viewpoints of fundamental research and technological applications. Their fascinating properties are naturally related to the crystallographic and electronic structures. Due to the covalent properties, the nitrides of Ti are technologically useful as, for instance, corrosion resistant coatings on cutting tools and diffusion barriers in silicon microcircuits [1–4]. It has been revealed that some properties of epitaxially grown TiN films are superior to those of polycrystalline ones. Thus, much interest has been focused on epitaxial films [5,6]. Recently, it was reported in the light of ex-situ experiments that NaCl-type TiN_y films were "epitaxially" grown by N-implantation into epitaxially deposited Ti films held at room temperature (RT) [7]. However, temperature dependence of the nitriding process of epitaxially deposited Ti films by N-implantation has not been sufficiently studied.

In this paper, changes of the crystallographic structures of epitaxially deposited Ti films during N-implantation were studied by using an in-situ transmission electron microscope (TEM).

2. Experimental

Detailed descriptions of the preparation method for deposited Ti films were presented in earlier papers [8,9]. Titanium films of 100 nm in thickness were deposited on NaCl (001) surfaces held at RT by an electron beam heating method in an ultra high vacuum. The Ti films separated from NaCl substrates were heated up to 350 °C at a heating rate of 2 °C/min in a 400 kV TEM combined with ion accelerators at JAERI-Takasaki [10]. The implantations of N_2^+ ions with 62 keV into Ti films held at 350 °C were performed in the TEM, in order to prevent Ti films from absorbing hydrogen atoms. According to a Monte Carlo simulation using the TRIM85 code, the projected range of N_2^+ with 62 keV was 55 nm. Thus, most of the implanted ions are to be retained inside Ti films. The N-concentrations in Ti films were evaluated from the implantation dose measured by a Faraday

* Corresponding author. Tel: +81-22-217-7775; fax: +81-22-217-7978.
E-mail address: kasukabe@insc.tohoku.ac.jp (Y. Kasukabe).

0040-6090/$ - see front matter © 2004 Elsevier B.V. All rights reserved.
doi:10.1016/j.tsf.2004.06.053

cage. The maximum dose in this experiment was 5.40×10^{17} ions/cm^2, which corresponded to the N/Ti ratio of 0.954 (the average atomic concentration of N in the Ti film).

3. Results and discussion

3.1. TEM observation

Fig. 1 shows typical electron diffraction (ED) patterns taken from (a) the as-deposited Ti film held at RT, (b) the Ti film held at 350 °C, and (c) the N-implanted Ti film (N/Ti = 0.954) held at 350 °C, respectively. An analysis of Fig. 1(a) elucidated that as-deposited Ti films consisted of (03·5)- and ($\bar{2}$1·0)-oriented hcp-Ti (lattice constants: a = 0.296 nm, c = 0.471 nm) and (110)-oriented CaF_2-type TiH_x ($x \cong 1.5$; lattice constant: a = 0.441 nm). The growth process of both hcp-Ti and TiH_x agrees with the results of previous papers [8,9]. The orientation relationships between the hcp-Ti and the NaCl substrate are (03·5) Ti//(001) NaCl and [2$\bar{1}$·0] Ti//[$\bar{1}$10] NaCl for (03·5)-oriented hcp-Ti, and ($\bar{2}$1·0) Ti//(001) NaCl and [00·1] Ti//[100] NaCl for ($\bar{2}$1·0)-oriented hcp-Ti. The (03·5)- and ($\bar{2}$1·0)-oriented hcp-Ti bring the 1$\bar{1}$·1 and 0$\bar{1}$·$\bar{1}$ reflections, respectively. Judging from the ED intensity, the growth of the (03·5)-oriented hcp-Ti is preferred to that of the ($\bar{2}$1·0)-oriented hcp-Ti. On the other hand, the orientation relationship between the TiH_x and NaCl is (110) TiH_x//(001) NaCl and [001] TiH_x//[110] NaCl for (110)-oriented TiH_x. The 002* and $\bar{1}$11* reflections in Fig. 1(a) stem from TiH_x in Ti films.

With increasing temperature, reflections of 002* and $\bar{1}$11* weakened gradually and disappeared completely at 350 °C, as shown in Fig. 1(b). On the other hand, ED intensities of the 1$\bar{1}$·1 and the 0$\bar{1}$·$\bar{1}$ reflections were slightly intensified, which indicates that the number of both the (03·5)- and the ($\bar{2}$1·0)-oriented hcp-Ti crystallites increases a little. These results show that H atoms which constitute TiH_x are completely released from it at 350 °C, and that all TiH_x crystallites have been transformed into hcp-Ti at 350 °C. The H-released unstable (110)-oriented fcc-Ti sublattices are transformed into hcp-Ti lattices with two kinds of orientation: one is (03·5)-oriented hcp-Ti, and the other is ($\bar{2}$1·0)-oriented hcp-Ti, as mentioned in Section 3.3. Analysis of the ED pattern in Fig. 1(c) elucidates that when N atoms are implanted into Ti films held at 350 °C, NaCl-type TiN_y crystallites with two kinds of orientation are formed: one is (001)-oriented TiN_y: (001) TiN_y//(001) NaCl and [100] TiN_y//[100] NaCl, and the other is (110)-oriented TiN_y: (110) TiN_y//(001) NaCl and [001] TiN_y//[110] NaCl. The (001)- and (110)-oriented TiN_y give rise to the 020 and $\bar{1}$11 reflections in Fig. 1(c), respectively. In the N-implanted Ti film (N/Ti = 0.954), there coexisted TiN_y (lattice constant: a = 0.424 nm) and a small amount of hcp-Ti (lattice constant: a = 0.296 nm, c = 0.485 nm). The orientation relationships of hcp-Ti are the same as those in as-deposited Ti films. The (03·5)-oriented hcp-Ti crystallites in Ti films held at 350 °C existed preferentially compared with the ($\bar{2}$1·0)-oriented hcp-Ti, while the formation of (001)-oriented TiN_y was preferred to that of (110)-oriented TiN_y in N-implanted Ti films held at 350 °C. Furthermore, it was found in the previous paper [11] that the nitrogen-implantation into the (03·5)-oriented hcp-Ti gives rise to the growth of only (001)-oriented TiN_y. Therefore, it can be considered that (001)-oriented and (110)-oriented TiN_y are "epitaxially" formed by the transformation of (03·5)-oriented and ($\bar{2}$1·0)-oriented hcp-Ti, respectively, as mentioned in Section 3.4.

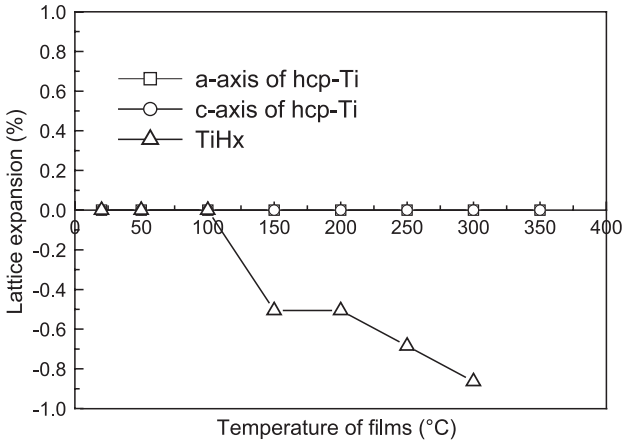

Fig. 2. Variation of lattice expansion with temperature of films.

3.2. Variation of the lattice constants

Fig. 2 shows the variation of the lattice expansions of hcp-Ti and TiH_x in the deposited Ti film, with increasing

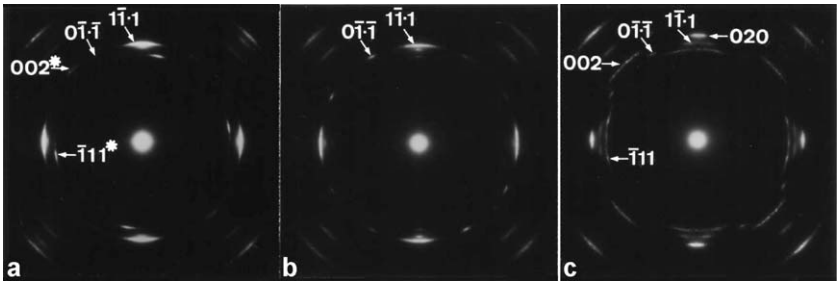

Fig. 1. Typical ED patterns taken from (a) as-deposited Ti film at RT, (b) Ti film held at 350 °C, and (c) N-implanted Ti film (N/Ti = 0.954) held at 350 °C.

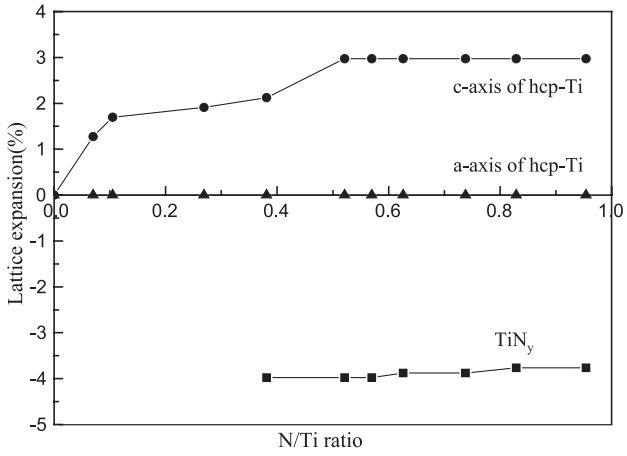

Fig. 3. Variation of lattice expansion with N/Ti ratio.

film temperature. The lattice expansion is defined as $100(a_T - a_0)/a_0$, where a_0 is a lattice constant of crystallites in as-deposited Ti films held at RT, and a_T is that in Ti films held at a temperature T. The lattice constant of TiH_x decreases gradually with the rise of temperature from 100 to 300 °C, which means that H atoms in the TiH_x are gradually released. This does not conflict with the previous paper [9]. On the other hand, there is no noticeable change of lattice constants of hcp-Ti up to 350 °C.

Fig. 3 shows the variation of the lattice expansions of hcp-Ti and TiN_y, with increasing N-dose. The lattice expansion is defined as $100(a_N - a_0)/a_0$, where a_0 is the same as in Fig. 2, and a_N is a lattice constant in N-implanted films. The lattice constant of TiH_x at RT is taken as a_0 for the evaluation of the lattice expansion of TiN_y. Since ED patterns of TiN_y with $N/Ti \leq 0.269$ were very weak and diffuse, the lattice constants of TiN_y could not be evaluated. The slight increase in the lattice constants of TiN_y with $N/Ti \geq 0.381$ results from the increase in the N concentration in TiN_y. Although the lattice expansion of the a-axis was difficult to detect, the lattice constant of the c-axis of hcp-Ti clearly increased with N-dose. This means that the c-axis of hcp-Ti lattice is expanded by the occupation of octahedral (O-) sites by N atoms [7,9,11]. Therefore, strain due to this lattice expansion can be considered as the major driving force for the hcp–fcc transformation of Ti sublattices.

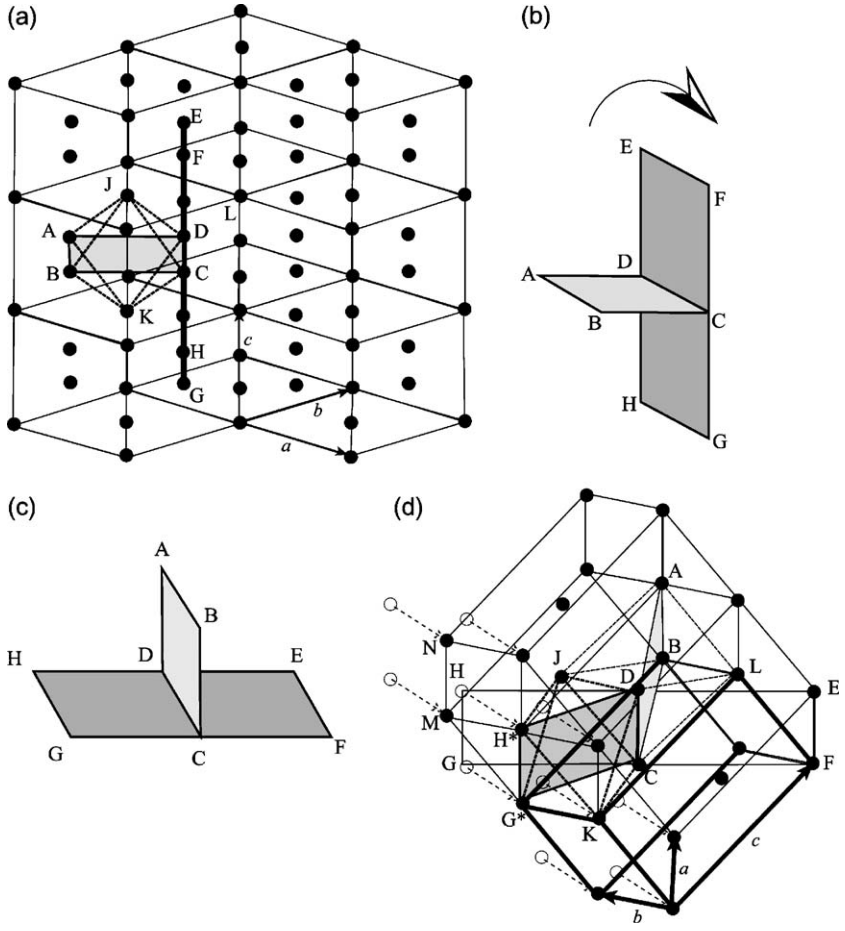

Fig. 4. Schematic illustration of transformation from (110)-oriented fcc-Ti to (03·5)-oriented hcp-Ti. (a) fcc-Ti, (b) ABCD (001) and EDHGCF {110} planes of fcc-Ti, (c) ABCD (03·$\bar{4}$) and EDHGCF (03·8) planes of hcp-Ti, (d) hcp-Ti. ● and ○ represent Ti atoms in each structure and Ti atoms of fcc-Ti before the transformation by the shear, respectively.

3.3. Transformation of TiH_x to hcp-Ti with the rise of temperature

Fig. 4 shows the orientation relationship between (110)-oriented fcc-Ti sublattice and (03·5)-oriented hcp-Ti structures. It should be noted that the occupation of tetrahedral sites of fcc-Ti sublattice by H atoms results in the formation of TiH_x. Fig. 4(a) and (d) illustrates schematically crystal structures of fcc-Ti and hcp-Ti sublattices, respectively. The rectangle GCFEDH in Fig. 4(b) corresponds to the projected line GHCDFE (in fact, a rectangle {110} plane of the fcc-Ti) in Fig. 4(a). Rotation of the rectangle GCFEDH in Fig. 4(b) about the CD axis by 90° gives rise to the rectangle GCFEDH in Fig. 4(c), which corresponds to the rectangle GCFEDH (03·8) plane of the hcp-Ti in Fig. 4(d). The G and H atoms shift to G* and H* positions in Fig. 4(d) by the fcc–hcp transformation. The direction of the shift is the MK direction $[0\bar{1}\cdot0]$ in Fig. 4(d). The (110) plane of fcc-sublattice, which is represented by the rectangle GCFEDH in Fig. 4(a) and (b), corresponds to the (03·8) plane of hcp-Ti, which is represented by the rectangle GCFEDH in Fig. 4(b) and (d). During and after the transformation, the square ABCD corresponds to the $(03\cdot\bar{4})$ plane of hcp-Ti, to ensure the inheritance of the octahedron JABCDL. When the shear occurs in the MK direction $[0\bar{1}\cdot0]$ in Fig. 4(d), the labeled H atom positioned at the center of gravity of the triangle MNH* and represented by an open circle, for example, has to be shifted to the H* site in order to form a hcp-Ti structure: open circles move to solid circles. Accordingly, the rectangle GCDH is transformed into the square G*CDH*, which gives rise to a JG*CDH*K octahedron. The G*CDH* plane is (03·4) plane of hcp-Ti. A dihedral angle of the (03·4) plane and the (03·5) plane, which is parallel to the film surface, is about 6.2°. Thus, the former is nearly parallel to the film surface. The hcp-Ti shown in Fig. 4(d) is called (03·5)-oriented hcp-Ti.

Similarly, Fig. 5 shows the orientation relationship between (110)-oriented fcc-Ti and $(\bar{2}1\cdot0)$-oriented hcp-Ti structures. Fig. 5(a) and (d) illustrates schematically crystal structure of fcc-Ti and hcp-Ti sublattices, respectively. The rectangle GAJIEDHC in Fig. 5(b) corresponds to the

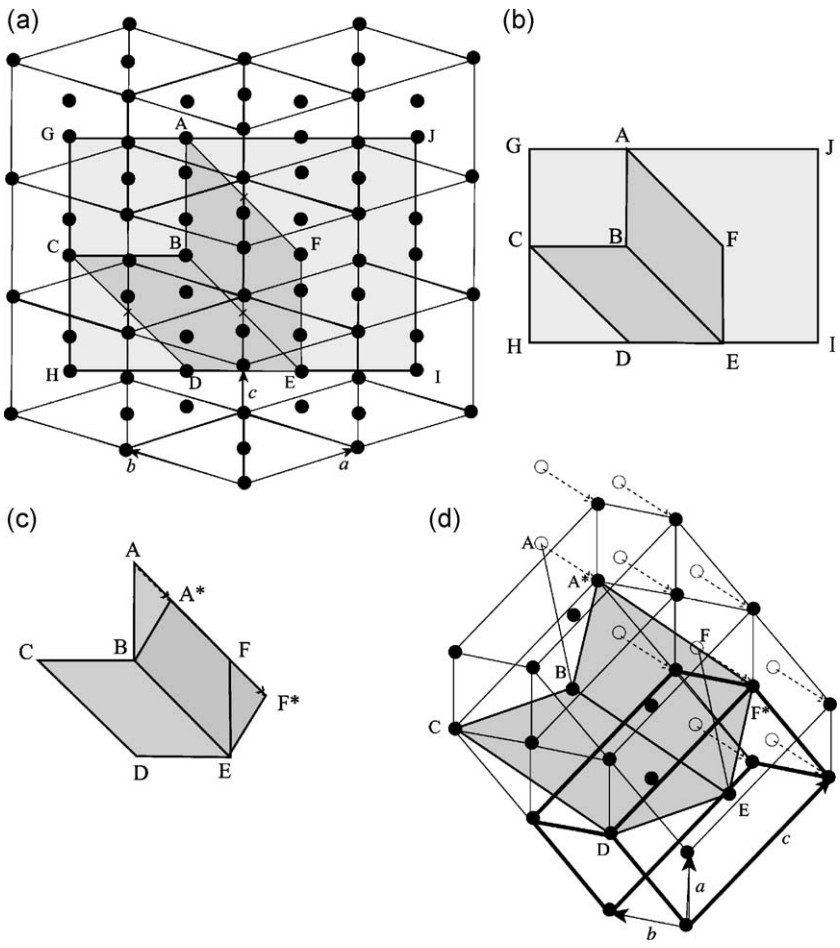

Fig. 5. Schematic illustration of transformation from (110)-oriented fcc-Ti to $(\bar{2}1\cdot0)$-oriented hcp-Ti. (a) fcc-Ti, (b) GCHDEIJA {110} plane of fcc-Ti, (c) A*BCDEF* $(\bar{2}1\cdot0)$ plane of hcp-Ti, (d) hcp-Ti. ● and ○ represent Ti atoms in each structure and Ti atoms of fcc-Ti before the transformation by the shear, respectively.

rectangle GAJIEDHC (110) plane in Fig. 5(a). The ABCDEF plane in Fig. 5(b) corresponds to the ABCDEF plane in Fig. 5(c). The fcc–hcp transformation leads A and F atoms to A* and F* positions in Fig. 5(c). The A*BCDEF* plane in Fig. 5(c) corresponds to the A*BCDEF* $(\bar{2}1{\cdot}0)$ plane in Fig. 5(d). In order to obtain the hcp-Ti structure, atoms indicated by open circles, such as A and F, in Fig. 5(d) have to be shifted to atoms indicated by solid circles such as A* and F*. Then, the direction of the shear is the AF direction $[0\bar{1}{\cdot}0]$ in the (00·1) plane of hcp-Ti. Thus, as shown in Fig. 5, the (110)-oriented fcc-Ti sublattice is transformed into $(\bar{2}1{\cdot}0)$-oriented hcp-Ti with increasing temperature.

3.4. Formation of TiN_y during N-implantation

Nitrogen-implantation into the Ti film at 350 °C results in the "epitaxial" growth of (001)-oriented and (110)-oriented TiN_y through the transformation of the hcp-Ti to fcc-Ti sublattice by partially inheriting the atomic arrangement of the hcp-Ti and accompanying the occupation of O-sites of the fcc-Ti by N atoms. It is considered that the (110)-oriented TiN_y is formed through the hcp–fcc transformation of Ti sublattice by inheriting the atomic arrangement BCDE of the $(\bar{2}1{\cdot}0)$-oriented hcp-Ti and shifting atoms indicated by solid circles such as A* and F* to positions indicated by open circles such as A and F in Fig. 5(d), which accompanies the occupation of O-sites of the fcc-Ti by N atoms. The previous study has revealed that the N-implantation into the (03·5)-oriented hcp-Ti leads to the "epitaxial" formation of the (001)-oriented TiN_y [11]. Therefore, the (001)-oriented TiN_y are formed through the transformation of (03·5)-oriented hcp-Ti to (001)-oriented fcc-Ti sublattice during the N-implantation, inheriting the JG*CDH*K octahedron as shown in Fig. 4(d), and by the occupation of O-sites of the (001)-oriented fcc-Ti by N. These analyses are consistent with the experimental results of previous papers [7–9,11]. The bonding interactions of Ti sublattices with N atoms have been studied in detail in the other paper [12], and it has been elucidated that the bonding interactions of Ti sublattices with N atoms give rise to the forming of stronger covalent bonds, which induces the weakening of Ti-Ti bonds. Thus, it is considered that the shear in the $\langle 01{\cdot}0\rangle$ direction of hcp-Ti induced by the forming of the strong Ti-N bonds and the weakening of the Ti–Ti bonds is the origin for the hcp–fcc transformation of Ti sublattice.

4. Conclusions

(1) Lattice constant of TiH_x decreases gradually with increasing film temperature. The ED pattern of TiH_x disappears at 350 °C. This indicates that the fcc-sublattice of TiH_x "epitaxially" transforms into hcp-Ti lattice with the release of H atoms, partially inheriting the atomic arrangement.
(2) When N-ions are implanted into Ti films at 350 °C, the lattice constant of the c-axis of hcp-Ti initially increases with the occupation of O-sites of hcp-Ti by N atoms.
(3) In the continued N-implantation at 350 °C, (001)-oriented and (110)-oriented TiN_y are "epitaxially" formed by the transformation of (03·5)- and $(\bar{2}1{\cdot}0)$-oriented hcp-Ti into fcc-sublattice, accompanying the occupation of O-sites of fcc-sublattice by N atoms, respectively.

Acknowledgements

This work was partially supported by a Grant-in Aid for Scientific Research from the Ministry of Education, Science and Culture of Japan.

References

[1] G.S. Chen, J.J. Guo, C.K. Lin, C.-S. Hsu, L.C. Yang, J.S. Fang, J. Vac. Sci. Technol., A 20 (2002) 479.
[2] J.E. Sundgren, Thin Solid Films 128 (1985) 21.
[3] R. Banerjee, K. Singh, P. Ayyub, M.K. Totlani, A.K. Suri, J. Vac. Sci. Technol., A 21 (2003) 310.
[4] C.-S. Shin, D. Gall, N. Hellgren, J. Patscheider, I. Petrov, J.E. Greene, J. Appl. Phys. 93 (2003) 6025.
[5] K. Sano, M. Oose, T. Kawakubo, Jpn. J. Appl. Phys. 34 (1995) 3266.
[6] J. Bøttiger, J. Chevallier, J.H. Petersen, N. Schell, W. Matz, A. Mücklich, J. Appl. Phys. 91 (2002) 5429.
[7] Y. Kasukabe, N. Saito, M. Suziki, Y. Yamada, Y. Fujino, S. Nagata, M. Kishimoto, S. Yamaguchi, J. Vac. Sci. Technol., A 16 (1998) 3366.
[8] Y. Kasukabe, J. Ootubo, S. Nagata, M. Kishimoto, Y. Fujino, S. Yamaguchi, Y. Yamada, Jpn. J. Appl. Phys. 34 (1995) 3234 (Part 1).
[9] Y. Kasukabe, S. Takeda, Y. Fujino, Y. Yamada, S. Nagata, M. Kishimoto, S. Yamaguchi, J. Vac. Sci. Technol., A 15 (1997) 1848.
[10] H. Abe, H. Naramoto, K. Hojou, S. Furuno, JAERI-Res. 96-047 (1996) 1.
[11] Y. Kasukabe, A. Ito, S. Nagata, M. Kishimoto, Y. Fujino, S. Yamaguchi, Y. Yamada, J. Vac. Sci. Technol., A 16 (1998) 483.
[12] Y. Kasukabe, J. J. Wang, T. Yamamura, S. Yamamoto, Y. Fujino, to be presented in ACSIN-7 and accepted for publication in "Thin Solid Films".